Stem Cell Reports
Article
ISSCR
OPEN ACCESS

Reprogramming astrocytes to motor neurons by activation of endogenous *Ngn2* and *Isl1*

Meiling Zhou,[1] Xiaoqing Tao,[1,2] Ming Sui,[1] Mengge Cui,[1] Dan Liu,[1] Beibei Wang,[1] Ting Wang,[1] Yunjie Zheng,[1] Juan Luo,[1] Yangling Mu,[1] Feng Wan,[3] Ling-Qiang Zhu,[4] and Bin Zhang[1,5,6,*]

[1]Department of Physiology, School of Basic Medicine, Tongji Medical College, Huazhong University of Science and Technology, Wuhan 430030, China
[2]Wuhan Institute of Biomedical Sciences, School of Medicine, Jianghan University, Wuhan 430056, China
[3]Department of Neurosurgery, Tongji Hospital, Huazhong University of Science and Technology, Wuhan 430030, China
[4]Department of Pathophysiology, School of Basic Medicine, Tongji Medical College, Huazhong University of Science and Technology, Wuhan 430030, China
[5]The Institute for Brain Research, Collaborative Innovation Center for Brain Science, Huazhong University of Science and Technology, Wuhan 430030, China
[6]Hubei Key Laboratory of Drug Target Research and Pharmacodynamic Evaluation, Huazhong University of Science and Technology, Wuhan 430030, China
*Correspondence: binzhang@hust.edu.cn
https://doi.org/10.1016/j.stemcr.2021.05.020

SUMMARY

Central nervous system injury and neurodegenerative diseases cause irreversible loss of neurons. Overexpression of exogenous specific transcription factors can reprogram somatic cells into functional neurons for regeneration and functional reconstruction. However, these practices are potentially problematic due to the integration of vectors into the host genome. Here, we showed that the activation of endogenous genes *Ngn2* and *Isl1* by CRISPRa enabled reprogramming of mouse spinal astrocytes and embryonic fibroblasts to motor neurons. These induced neurons showed motor neuronal morphology and exhibited electrophysiological activities. Furthermore, astrocytes in the spinal cord of the adult mouse can be converted into motor neurons by this approach with high efficiency. These results demonstrate that the activation of endogenous genes is sufficient to induce astrocytes into functional motor neurons *in vitro* and *in vivo*. This direct neuronal reprogramming approach may provide a novel potential therapeutic strategy for treating neurodegenerative diseases and spinal cord injury.

INTRODUCTION

Injury to the human central nervous system (CNS) is devastating because our adult CNS has little regenerative capacity to replace lost neurons and induce functional recovery. Hence, acute CNS injury and chronic neurodegenerative diseases are associated with irreversible loss of neurons, ultimately leading to permanent functional deficit and neurological disability. The ultimate goal of regenerative medicine for CNS injury repair is to replace lost neurons to restore lost functions. One common type of CNS injury is spinal cord injury (SCI). With the development of the economy, the incidence of SCI is increasing gradually. There are from 250,000 to 500,000 people around the world suffering from SCI every year according to recent World Health Organization reports (Courtine and Sofroniew, 2019; Fehlings et al., 2017). SCI leads to irreversible neuron loss and the interruption of the ascending and descending spinal tract, leading to sensory and motor dysfunction below the injury plane and even severe disability (Bradbury and McMahon, 2006; Thuret et al., 2006). The clinical symptoms related to SCI depend on the anatomical level and severity of the lesion, ranging from mild sensory/motor disorders to complete quadriplegia (Noristani et al., 2016), which brings a heavy burden to the family and society. After SCI, astrocytes proliferate to form a dense glial scar in the injured site, which forms a physical barrier to prevent axonal regrowth (Fawcett and Asher, 1999; Noristani et al., 2016; Yiu and He, 2006). So far, there is barely an effective strategy for promoting the recovery of function in the clinic. Due to the limited self-healing ability of the CNS after injury, many defects remain permanent. Therefore, nerve repair and locomotor functional reconstruction after SCI are the most challenging medical problems.

Cell replacement is a potential therapeutic strategy for the loss of neurons after injury (Gong et al., 2020; Snyder and Teng, 2012). Although this therapy can compensate for motor neuron (MN) loss after SCI, the sources of functional MNs are still limited. Recent studies showed the generation of MNs from induced pluripotent stem cells (iPSCs) (Chen et al., 2014; Fernandopulle et al., 2018); however, cellular therapy still faces several significant obstacles in treating human SCI. First, the generation of iPSCs and their gradual differentiation into MNs is a long and complicated process, which is technically challenging due to the variable lineage of iPSCs and the heterogeneity of differentiated neurons (Arbab et al., 2014; Liu et al., 2016). Second, transplanting cells of this origin may increase the risk of tumor formation (Knoepfler, 2009). Third, the transplantation process may lead to secondary SCI. Furthermore, cell transplantation often requires a large number of cells, which may result in unexpected damage to the pre-existing functional neural circuits and the formation of cystic tissue at the injection site (Su et al., 2014).

More recent studies have shown that defined transcription factors (TFs) can directly induce fibroblasts or astrocytes into functional neurons, which further proves the feasibility of direct transdifferentiation of non-neuronal cells into neurons. For example, mouse cortical astrocytes can be converted into glutamatergic and GABAergic neurons by overexpression of *Ngn2* and *Dlx2*, respectively (Heinrich et al., 2010). Dopaminergic neurons can be generated from mouse and human fibroblasts by overexpression of three TFs: *Ascl1*, *Nurr1*, and *Lmx1α* (Caiazzo et al., 2011). Overexpressing defined TFs can induce serotonergic neurons from human fibroblasts (Vadodaria et al., 2016; Xu et al., 2016). Small molecules combined with overexpression of *Ngn2* can convert human fibroblasts to cholinergic neurons (Liu et al., 2013). The knockdown of *Ptbp1* promotes the glial-to-retinal ganglion cell or astrocyte-to-dopaminergic neuron conversion in a Parkinson's disease mouse model (Qian et al., 2020; Zhou et al., 2020). However, the generation of MNs by direct neuronal reprogramming has been barely reported. Recent progress in direct neuronal reprogramming revealed that induced neurons (iNs) could be used in cellular therapy as well as disease modeling (Drouin-Ouellet et al., 2017; Furlan et al., 2016; Li et al., 2019; Liu et al., 2016; Qian et al., 2020). Despite the limitations of reprogramming efficiency and neuron purity, the directly transformed specific neurons may still be valuable for disease modeling and drug identification of late-onset human nervous system diseases (Arbab et al., 2014).

Recently, the type II clustered regularly interspaced short palindromic repeat and Cas9 nuclease (CRISPR/Cas9) system from bacteria was repurposed for genome editing in mammalian cells (Cong et al., 2013; Mali et al., 2013). Dead Cas9 (dCas9), an inactivated form of Cas9, has been designed to fuse with transactivation factor to form programmable synthetic TFs, known as the CRISPR activation (CRISPRa) system (Konermann et al., 2015; Zalatan et al., 2015). This system can function as a pioneer factor to target the silenced chromatin locus with high accuracy and promote downstream gene transcription (Liu et al., 2018; Polstein et al., 2015). Our study explores the possibility of direct reprogramming of the astrocytes and mouse embryonic fibroblasts (MEFs) into MNs by gene editing. In this study, using the CRISPRa system, we provide an easy-to-follow approach for direct and highly efficient conversion of mouse spinal cord astrocytes and MEFs into functionally mature MNs *in vitro* and *in vivo*.

RESULTS

Activation of endogenous *Ngn2* and *Isl1* with dCas9-VP64

It has been reported that overexpression of the TFs Islet-1 (*Isl1*) and LIM Homeobox 3 (*Lhx3*) along with neurogenin 2 (*Ngn2*) can differentiate iPSCs into lower MNs (Fernandopulle et al., 2018). We wondered whether spinal cord astrocytes could be reprogrammed into functional MNs by TF combinations. The CRISPRa system was used to activate the expression of endogenous genes (Konermann et al., 2015), and single-guide RNAs (sgRNAs) were designed to target the *Ngn2* and *Isl1* promoter region close to the transcription start site. *Ngn2* was chosen for its ability to convert astrocytes into functional iNs, and *Isl1* is an important TF for MN specification. We first detected transcriptional activation of target genes with each designed *Ngn2* and *Isl1* sgRNA delivered by lentivirus in primary cultured astrocytes. Gene expression analysis showed that sgRNAs targeting the promoter of *Ngn2* induced a 20-fold upregulation of *Ngn2* transcription. For *Isl1* promoter, about a 10-fold increase was observed (Figure S1A). The increased protein expressions of NGN2 and ISL1 in astrocytes by sgRNAs were also verified by western blot (Figures S1B and S1C). Designed sgRNAs and the dCas9-VP64-GFP plasmids were also transduced into MEFs to verify the transcriptional activation of target genes (data not shown). These results suggest that dCas9-VP64 can activate the silenced *Ngn2* and *Isl1* in astrocytes through specific sgRNA guidance.

Activation of *Ngn2* and *Isl1* enabled mouse spinal cord astrocytes to acquire motor neuronal properties

To explore whether spinal cord astrocytes can be induced into functional MNs through activation of endogenous *Ngn2* and *Isl1*, we isolated astrocytes from the spinal cord of neonatal C57/BL6J mice (postnatal days 0–3) and cultured them as initiating cells for reprogramming. Primary astrocytes were cultured to the third generation to remove residual neurons, and about 95% of the cells expressed the astrocyte marker glial fibrillary acidic protein (GFAP). The cultured cells showed almost no expression of the neuronal marker MAP2 or motor neuronal marker HB9, nor microglia marker IBA1 (Figures 1A, 1B, and S1D). These results indicated that the cultured cells were astrocytes with undetectable neurons or microglial cells. We first examined whether activation of endogenous *Ngn2* and *Isl1* could induce astrocytes into MNs by being infected with the lentivirus dCas9-VP64-GFP and the sgRNA. The date of infection was denoted as day 0, and the medium was switched to neuronal medium containing 2% B27 supplement on day 3 (Figure 1C). During the process of conversion, cell morphology changed from an initially flat, spread-out shape to one with bipolar and multipolar processes and smaller cell bodies, showing typical complex neurite-like structures. At 14 days post infection (dpi), we added a ROCK inhibitor, Y-27632, to promote the neurite extension as suggested by a previous study (Klim et al., 2019). At 18 dpi, the induced cells exhibited typical neuronal morphology (Figure 1D). Immunostaining results

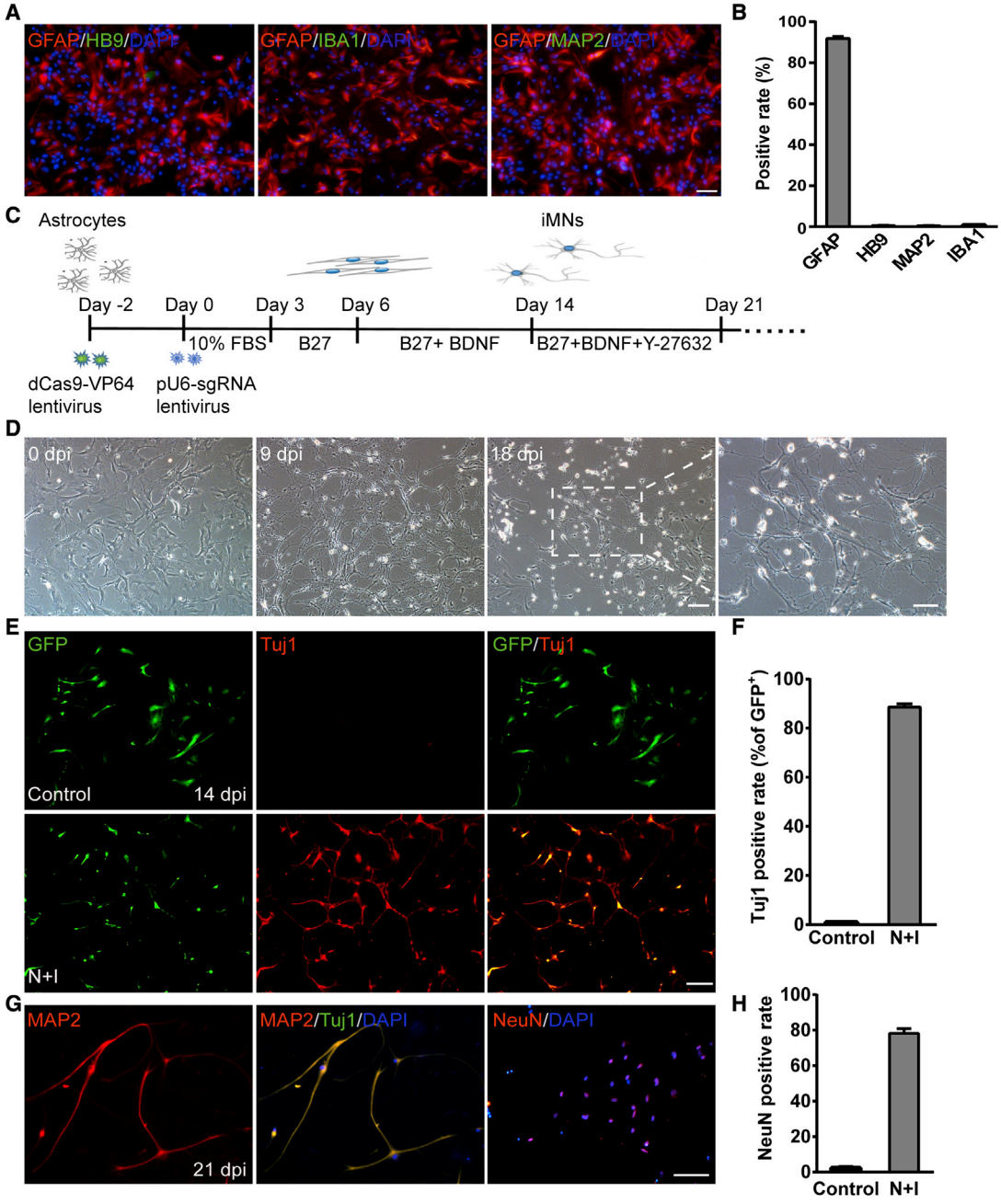

Figure 1. Conversion of astrocytes into induced neurons (iNs)

(A) The cultured astrocytes at passage 3 expressed GFAP but almost no expression of MAP2, HB9, and IBA1. Scale bar, 50 μm.

(B) Quantitative analysis of (A) (n = 3 independent experiments).

(C) Timeline for the reprogramming process.

(D) Cell morphology during the reprogramming. Scale bar, 100 μm. Right: image of iNs at high magnification. Scale bar, 50 μm.

(E) Representative images showing the expression of the neuronal marker Tuj1 at 14 days post infection (dpi). GFP indicated the virus-transduced cells. Scale bars, 100 μm.

(F) Reprogramming efficiency is determined by the percentage of $Tuj1^+$ cells relative to GFP^+ cells at 14 dpi (n = 4 independent experiments).

(G) iNs expressed the mature neuronal markers MAP2 and NeuN at 21 dpi. Scale bar, 50 μm.

(H) Quantitative analysis of $NeuN^+$ cells relative to GFP^+ cells (n = 4 independent experiments). Data are presented as mean ± SEM.

revealed that the neuronal marker Tuj1 became detectable at 14 dpi, and about 88% of virus-transduced astrocytes converted into Tuj1$^+$ cells. However, the expression of Tuj1 was almost undetectable in the control group, even within the GFP-positive cells (Figures 1E and 1F). Since Tuj1 is expressed in both immature and mature neurons, its expression per se during *Ngn2-Isl1*-induced neurogenesis does not indicate the maturation of the induced neurons. Instead, MAP2 and NeuN are widely used as markers for mature neurons. We detected these markers at 21 dpi during *Ngn2-Isl1*-induced neurogenesis with a relatively high rate (78.2% ± 2.7% for NeuN$^+$, n = 4) (Figures 1G and 1H). These data indicate that *Ngn2-Isl1*-induced neurons could mature *in vitro*.

We next examined the mRNA expressions of some marker genes of astrocyte and neuron. As shown in Figure S2, the expression of *Aldh1l1* and *Gfap*, two astrocyte-specific genes, gradually decreased during the conversion by *Ngn2* and *Isl1* activation, while *NeuroD4*, a neuron-specific marker, showed elevated expression level by day 7, and eventually achieved an almost 10-fold increase by day 14. One mechanism of gene expression regulation of *Gfap* is DNA methylation in the promoter region in neurons at the neurogenic stage during normal development (Condorelli et al., 1997; Teter et al., 1996). We thus assessed the methylation levels of *Gfap* in the promoter region by sequencing-based bisulfite sequencing PCR (BSP). The results showed that the methylation level of all CpG sites in promoter regions increased, and the median methylation level significantly increased from 63.6% to 82% during the process of conversion (Figures S3A and S3B). These data indicate that the reduction of *Gfap* could be caused by the hypermethylation in the promoter region upon reprogramming.

Next, we analyzed the subtype properties of reprogrammed neurons. Immunostaining results revealed that the induced cells expressed spinal MN marker HB9, and over 83% of Tuj1$^+$ cells co-stained with HB9 at 14 dpi (Figures 2A and 2B). The induced neuronal cells also expressed the cholinergic MN marker choline acetyltransferase (ChAT). Immunofluorescence quantitative analysis displayed that almost 70% of Tuj1$^+$ cells expressed ChAT (Figures 2C and 2D). In contrast, none of the induced neuronal cells expressed GAD1, a marker for GABAergic neurons (Figure 2E). When co-cultured with mouse astrocytes, the induced neurons survived over 35 days with the continuous expression of HB9 (Figure 2F). It is well known that the distinct Hox gene expression pattern along the rostrocaudal axis confers regional neuronal identity in the spinal cord. To further specify the nature of the induced neuron, we examined the mRNA expressions of region-specific Hox genes. We found that *Hoxc6* (brachial region), *Hoxc8* (brachial region), *Hoxc9* (thoracic region), and *Hoxc10* (lumbar region) were upregulated significantly by 14 days of *Ngn2* and *Isl1* activation (Figure S2C), showing no regional specificity of the induced neurons. These results suggest that the cultured astrocytes mainly acquired a motor neuronal fate after activation of endogenous *Ngn2* and *Isl1*.

We then examined whether the induced motor neurons (iMNs) were functional. We found that the iMNs with typical neuronal morphology also expressed the presynaptic marker synaptotagmin 1 (SYT1) with a punctate pattern, suggesting the establishment of synaptic structures, at 21 dpi. Quantitative analysis revealed that over 58% of Tuj1$^+$ cells could be co-stained with SYT1 (Figures 2G and 2H). Electrophysiological characteristics of induced neurons were detected by whole-cell patch clamp. The induced GFP$^+$ neuronal cells showed typical spontaneous postsynaptic currents (sPSCs) at 35 dpi. More importantly, sPSCs could be blocked by 10 μM CNQX, an antagonist of AMPA/kainate glutamate receptors (Figures 2I and 2J; n = 3 of 12 cells). The induced neuronal cells could fire repetitive action potentials (APs) in response to the injection of step currents, and APs could be eliminated by blocking voltage-gated sodium channels with1 μM tetrodotoxin (TTX) (Figure 2K; n = 5 of 14 cells). Together, these data indicated that iMNs could generate electrophysiological activities and form synaptic connections.

Conversion of MEFs to functional motor neurons by activation of *Ngn2* and *Isl1*

The above results showed that activation of *Ngn2* and *Isl1* can induce postnatal mouse spinal cord astrocytes into functional MNs. We then wondered whether MEFs could be reprogrammed into iMNs in the same way, as fibroblasts are widely used as the starting cells for neuron reprogramming (Herdy et al., 2019; Li et al., 2019; Son et al., 2011; Vierbuchen et al., 2010). MEFs were isolated from wild-type mice and infected with dCas9-VP64-GFP and the sgRNA lentivirus. At 14 dpi, 83% of virus-transduced MEFs were found to be positive for Tuj1 (Figure 3A). Meanwhile, about 80% of Tuj1$^+$ reprogrammed cells expressed HB9 (Figure 3B). Furthermore, the reprogrammed cells also expressed the pan-neuronal marker MAP2 (Figure 3C) as well as the cholinergic MN marker ChAT at 21 dpi (64.3% ± 3.3% for ChAT$^+$ of Tuj1$^+$ cells, n = 3, Figure 3D). These cells exhibited typical MN morphology with multiple dendrites and prominent axons. These data suggested that MEFs could be efficiently converted into iMNs by activation of *Ngn2* and *Isl1* as well.

Next, we analyzed the functional characteristics of iMNs derived from MEFs. Immunostaining results revealed that the converted cells also expressed the presynaptic marker SYT1 at 21 dpi, and almost 60% of Tuj1$^+$ cells co-stained with SYT1 (Figure 3E). The electrophysiological properties of iMNs derived from MEFs were examined at 35 dpi and

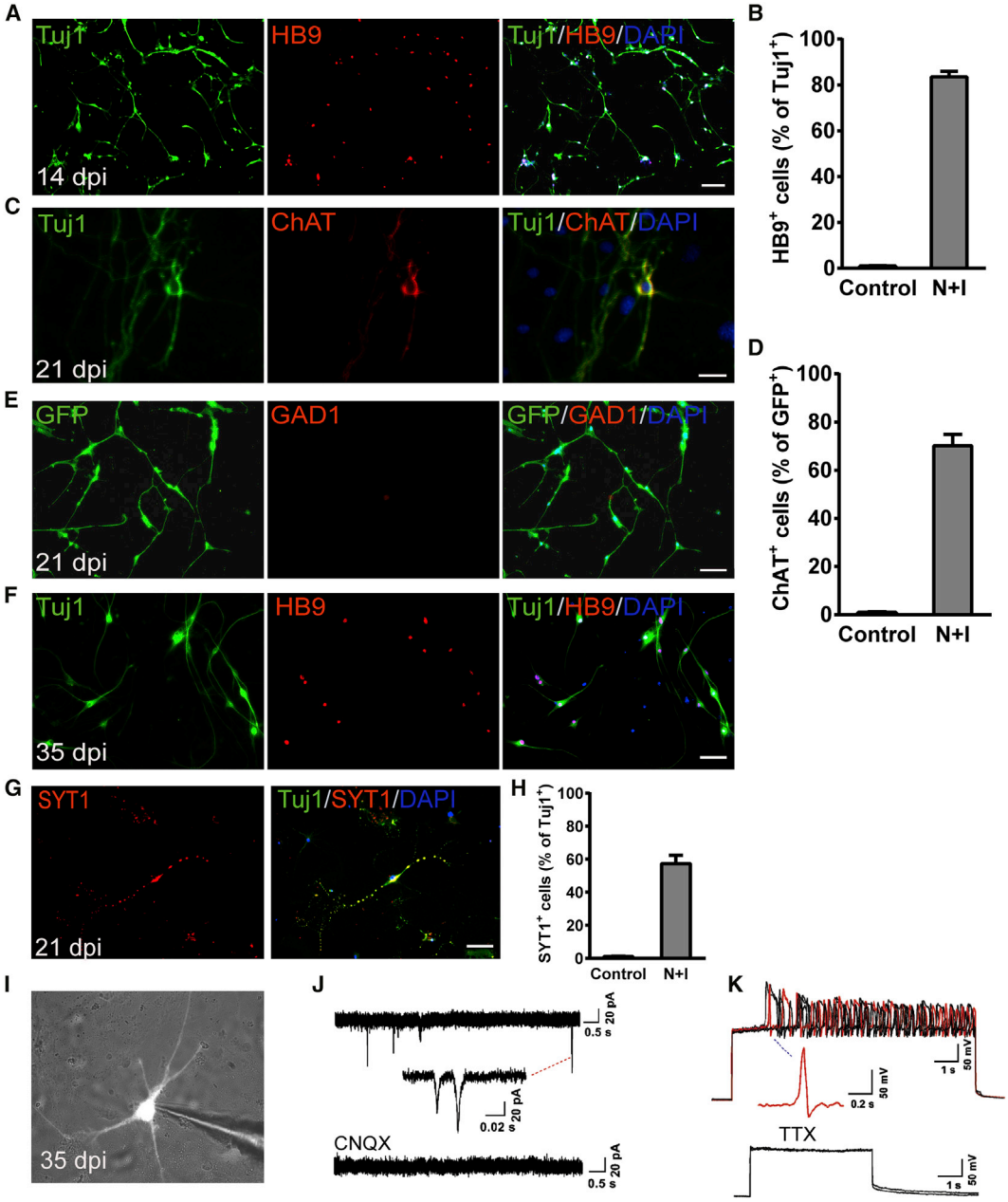

Figure 2. iNs showed motor neuronal properties

(A) Motor neuron marker HB9 expression in mouse spinal cord astrocyte-derived iNs at 14 dpi. Scale bar, 100 μm.

(B–E) (B) Neuronal purity is determined by the expression of HB9 relative to Tuj1$^+$ cells at 14 dpi (n = 4 independent experiments). Immunostaining with (C) ChAT and (E) GAD1 antibodies at 21 dpi. Scale bars, 50 μm. (D) Quantitative analysis of ChAT$^+$ cells relative to Tuj1$^+$ cells (n = 4 independent experiments). Data are presented as mean ± SEM.

(F) iMNs morphology and expression of HB9 at 35 dpi. Scale bar, 50 μm.

(G and H) (G) iMNs expressed the presynaptic marker SYT1 and at 21 dpi. Scale bar, 50 μm. (H) Quantification of (G) (n = 3 independent experiments). Data are presented as mean ± SEM.

(I) Patch-clamp recordings were performed on iMNs at 35 dpi.

(J) Representative traces of spontaneous postsynaptic currents were recorded from iMNs under the voltage-clamp mode and could be blocked by CNQX (n = 3 of 12 cells).

(K) Representative traces of APs recorded from iMNs when injected with step currents, which could be blocked by the Na$^+$ channel blocker tetrodotoxin (TTX). An exemplary trace is highlighted in red (n = 5 of 14 cells).

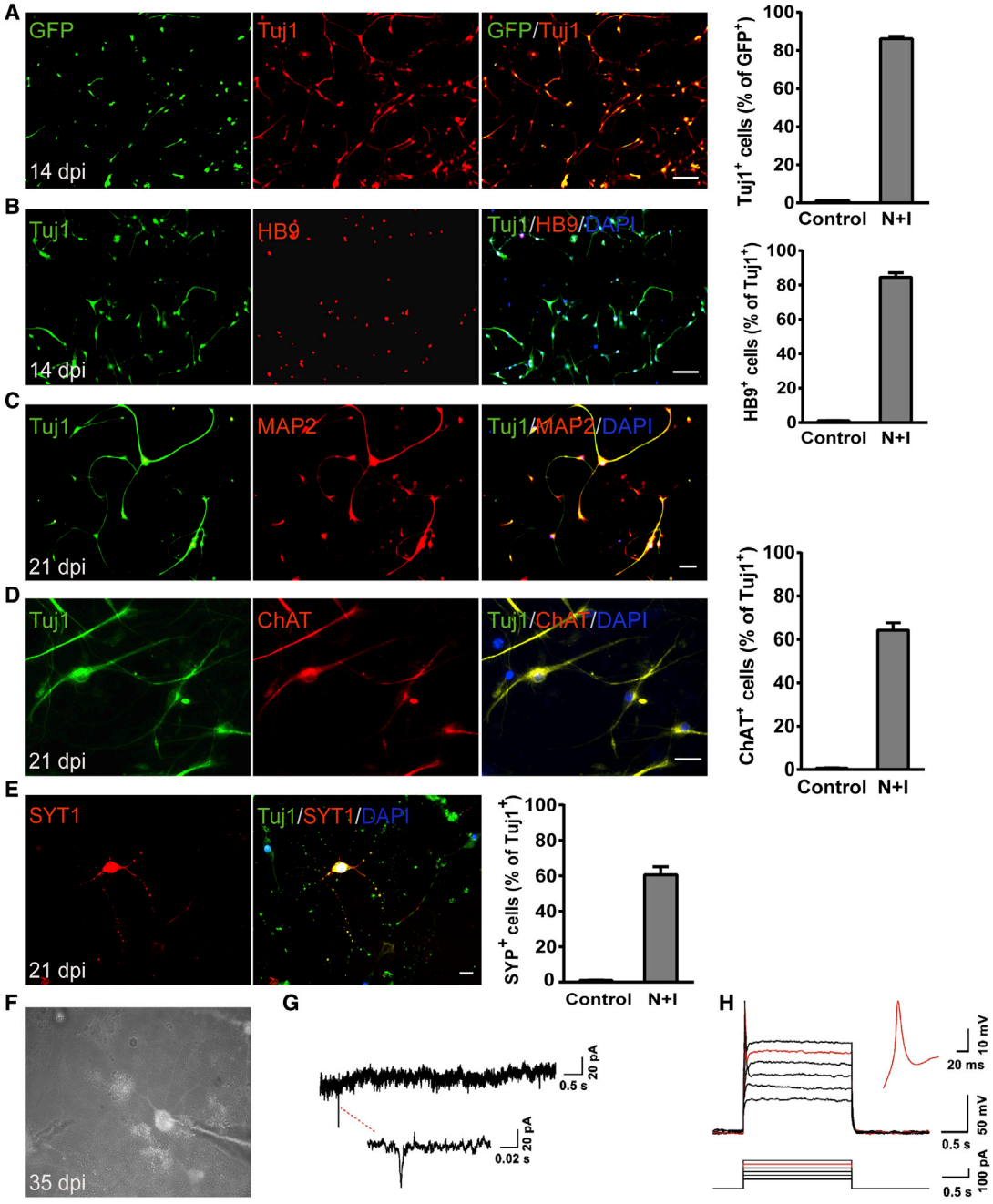

Figure 3. Conversion of MEFs to functional MNs

(A) Representative images showing the expression of the neuronal marker Tuj1 at 14 dpi (n = 4 independent experiments). GFP indicated the virus-transduced cells. Scale bar, 100 μm. Reprogramming efficiency is determined by the percentage of $Tuj1^+$ cells relative to GFP^+ cells at 14 dpi.

(B) iMNs derived from MEFs expressed HB9 at 14 dpi (n = 4 independent experiments). Scale bar, 100 μm. Neuronal purity is determined by the expression of motor neuron marker HB9.

(C and D) iMNs expressed (C) the mature neuronal marker MAP2 and (D) the cholinergic motor neuron marker ChAT at 21 dpi (n = 3 independent experiments). Scale bars, 50 μm (C) and 20 μm (D).

(E) iMNs expressed the presynaptic marker SYT1 at 21 dpi (n = 3 independent experiments). Scale bar, 50 μm.

(F) Patch-clamp recordings were performed on iMNs at 35 dpi.

(legend continued on next page)

beyond. Whole-cell patch-clamp recordings showed that robust sPSCs could be detected at 35 dpi (Figures 3F and 3G). In response to the injection of step currents, iMNs could fire repetitive APs (Figure 3H; n = 5 of 12 cells). Thus, iMNs derived from MEFs became mature in terms of electrophysiological function.

In vivo conversion of spinal cord astrocytes of adult mice into neurons by activation of endogenous *Ngn2* and *Isl1*

After successfully establishing astrocyte-to-neuron conversion *in vitro*, we next investigated whether astrocytes could be converted into neurons in the mouse spinal cord by activation of *Ngn2* and *Isl1*. AAV has a high infection rate and low pathogenicity and has been approved by the US Food and Drug Administration for clinical trials of the treatment of CNS diseases (Chen et al., 2020). In particular, AAV9 has emerged as one of the most commonly used serotypes in the nervous system for its ability to cross the blood-brain barrier and be widely distributed in the brain and spinal cord, targeting neurons and astrocytes (Bailey et al., 2020; Lykken et al., 2018). We chose the recombinant AAV9 vectors to deliver dCas9-VP64 and the sgRNAs targeting *Ngn2* and *Isl1* into the mouse spinal cord. sgRNAs targeting *Ngn2* and *Isl1* were constructed under the direct control of U6 and mU6 promoter, respectively. The AAV-dCas9-VP64-EGFP vector contained the cytomegalovirus promoter and the coding sequence for dCas9-VP64 fused with 2A-EGFP (Figure S4A). To track the astrocyte-converted neurons in the mouse spinal cord, we used astrocyte-specific reporter mouse strain, hGFAP-CreERT2;Rosa26-CAG-tdTomato, which expresses tdTomato (tdT) specifically in astrocytes. This mouse strain was generated by crossing hGFAP-CreERT2 transgenic mice with conditional Rosa26-CAG-tdTomato reporter mice (Figure S4B). Once stimulated by tamoxifen, Cre recombinase, under the control of the human GFAP promoter, translocates into nucleus and induces the expression of tdT. We examined the identity of the labeled cells (tdT^+ cells, red) in the adult spinal cord and found that 96.3% of the tdT^+ cells expressed the astrocyte marker GFAP, while fewer than 2% were positive for the neuronal markers NeuN (Figures S5A and S5B), suggesting a reasonably low degree of leakage of the GFAP-Cre expression.

We first injected AAV-dCas9-VP64-EGFP into the spinal cord to test the infection efficiency. We found that the expression of GFP became evident 14 days post AAV injection (14 dpi). It is remarkable that although AAV9 can infect both astrocytes and neurons, only ~12% of GFP^+ cells expressed the neuronal marker NeuN, and most of the GFP^+ cells expressed the astrocyte marker GFAP in our study (data not shown). AAV-sgRNAs (AAV-N + I) and AAV-dCas9-VP64-EGFP virus were then co-injected into the T10 region of the adult spinal cord of hGFAP-CreERT2;Rosa26-CAG-tdTomato mice (age 2–4 months) and analyzed for induced neurogenesis at different time points (Figure 4A). For the control group, mice were co-injected with AAV-sgRNA empty vector virus. At 14 dpi, AAV-N + I/GFP-infected tdT^+ cells (GFP^+/tdT^+) were mainly $GFAP^+$ astrocytes, and the neuronal marker NeuN was almost not detected, suggesting that the virus-infected astrocytes had not yet been converted into neurons (Figures 4B and S6A). At 28 dpi, immunostaining showed that AAV-N + I/GFP-infected tdT^+ cells became NeuN-positive neurons; these $GFP^+/tdT^+/NeuN^+$ cells were astrocyte-converted neurons. Quantitative analyses revealed that about 28.3% of AAV-N + I/GFP-infected tdT^+ cells acquired neuronal identity, and the percentage of neuronal conversion continuously increased to 43.2% at 42 dpi (Figures 4C and 4D). Parallel to this trend, a growing number of GFP^+/tdT^+ cells co-localized with NeuN, while the number of GFP^+/tdT^+ cells co-localized with GFAP ($GFAP^+$) reduced from 94.3% at 14 dpi to 46.8% at 42 dpi (Figures S6A–S6D). Conversely, in the control group, AAV/GFP-infected tdT^+ cells scarcely expressed NeuN (Figures 4B–4D). These results indicated that activation of *Ngn2* and *Isl1* could convert spinal cord astrocytes into neurons *in vivo*. We next investigated the neuronal subtypes generated from astrocyte-to-neuron conversion. Immunostaining results showed that nearly half of GFP^+/tdT^+ cells (42 dpi) were $HB9^+$ (49.7% ± 4.3%, n = 4) or $ChAT^+$ (44.5% ± 3.6%, n = 4) MNs (Figures 5A–5C and 5F) with almost no expression of GABAergic marker GAD1 (Figures 5E and 5F). Quantitative analysis of the MN population in the virus-injected core areas revealed that the motor neuronal density in the control group was 16.1 ± 1.2/0.01 mm^2, whereas, in the N + I group MNs reached 28.7 ± 1.5/0.01 mm^2 (Figure 5D, n = 4), which may be attributed to astrocyte-to-MN conversion. These results demonstrated that activation of endogenous *Ngn2* and *Isl1* could efficiently convert astrocytes into MNs in the adult spinal cord.

Astrocytes in the white matter of the spinal cord fail to reprogram to neurons

Considering the specificity and maturity of iMNs in the gray matter (GM), strikingly we found that there were no $GFP^+/tdT^+/NeuN^+$ cells in the white matter (WM) at 42 dpi, although double-positive cells (GFP^+/tdT^+) could be

(G) Representative traces of spontaneous postsynaptic currents were recorded from iMNs under voltage-clamp mode.
(H) Representative traces of APs recorded from iMNs when injected with step currents. An exemplary trace is highlighted in red (n = 5 of 12 cells).
Data are presented as mean ± SEM.

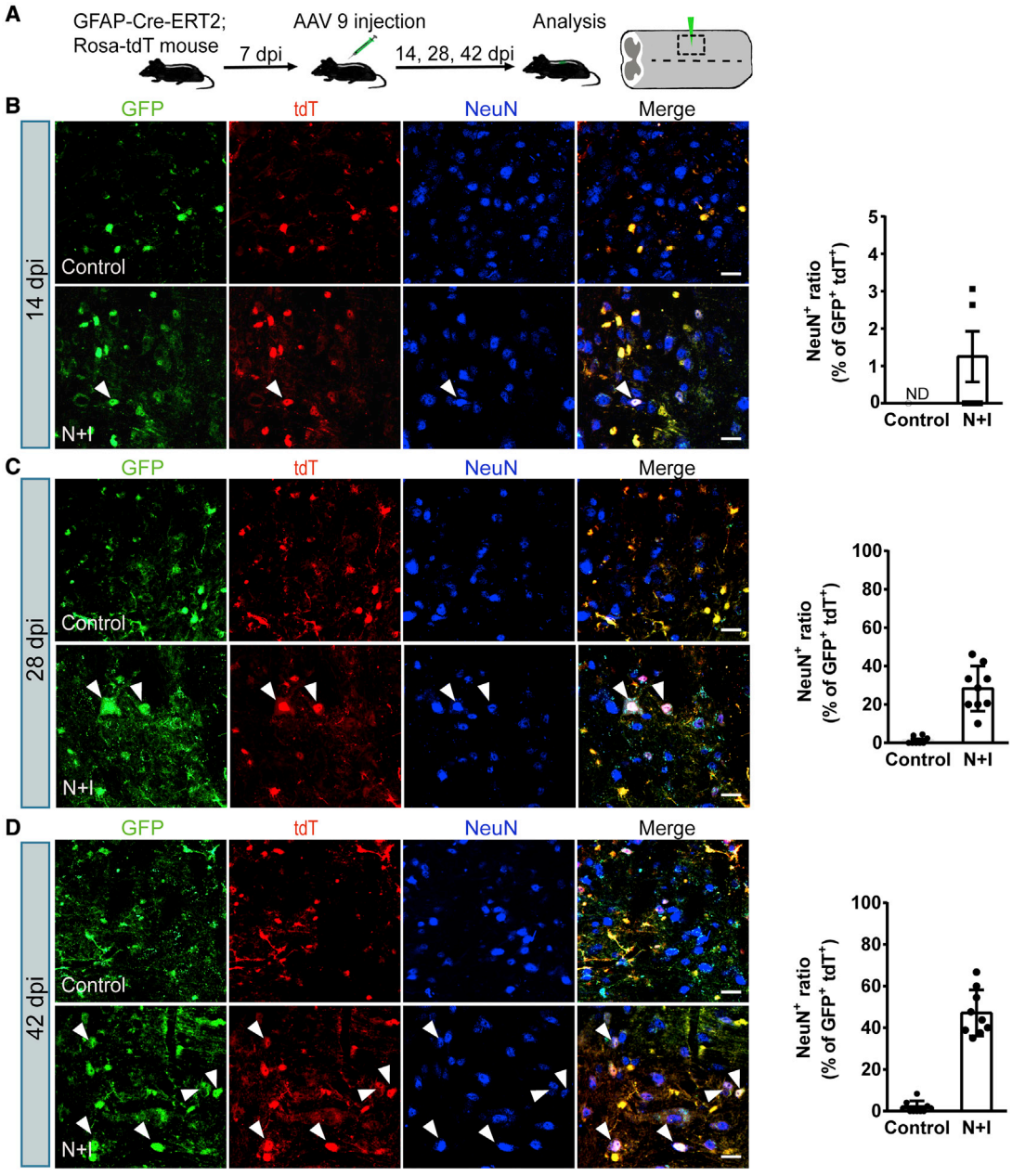

Figure 4. *In vivo* conversion of spinal cord astrocytes into neurons in GFAP-CreERT2;Ai14 transgenic mouse

(A) Outline of experimental design.

(B–D) Representative images showing the expression of the neuronal marker NeuN at (B) 14 dpi, (C) 28 dpi, and (D) 42 dpi, and quantifications of NeuN$^+$ cells among all viral infected tdT$^+$ cells (n = 5 independent experiments). Arrowheads indicate the converted neurons. ND, not detected. Scale bars, 20 μm. Data are presented as mean ± SEM.

identified in that area (Figure 6A). To further verify this result, we examined the WM area and found double-positive cells (GFP$^+$/tdT$^+$) throughout the WM, indicating efficient targeting of WM astrocytes. However, no GFP$^+$/tdT$^+$/NeuN$^+$ cells were detectable (Figure 6B). On the contrary, more than 50% of the double GFP$^+$/tdT$^+$ cells were NeuN$^+$ cells in the GM (Figure 6C). These results indicated that WM astrocytes fail to reprogram to neurons, even if the same TFs are activated.

Converted motor neurons project into sciatic nerves

Lower MNs in the spinal cord project axons into skeletal muscles to control muscle excitation and contraction. Next, we investigated whether the induced MNs can

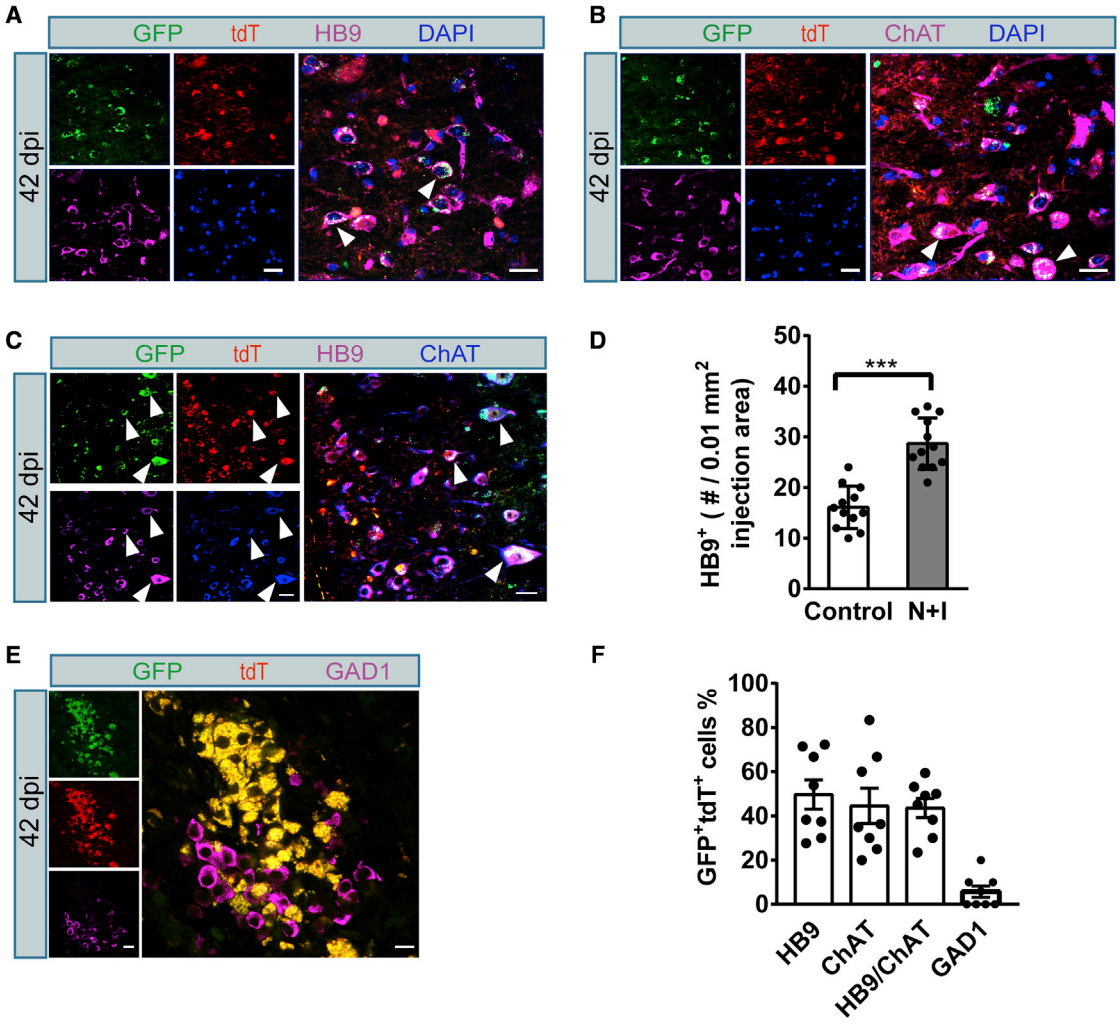

Figure 5. Converted neurons generated from astrocytes showed motor neuron features in the spinal cord of adult hGFAP-CreERT2;Ai14 transgenic mouse

(A, B, C, E) Representative images showing converted neurons co-stained with (A) HB9, (B) ChAT, (C) HB9/ChAT double-labeled staining, and (E) GAD1 after activation of endogenous *Ngn2* and *Isl1* in spinal cord astrocytes (42 dpi). Arrowheads indicate co-labeled cells. Scale bars, 20 μm.

(D) Quantification of total $HB9^+$ cells in the virus-injected core areas of control group and N + I group (n = 4 independent experiments). Data are presented as mean ± SEM ***p < 0.0001.

(F) Quantified data showing the composition of the astrocyte-converted neurons (n = 4 independent experiments). Data are presented as mean ± SEM.

project into natural target muscles. To this end, we collected sciatic nerves from AAV-N + I-infected mice at 42 dpi and examined the existence of iMN axons. Longitudinal sections and cross-sections revealed that iMN projected axons (GFP^+/tdT^+) in AAV-N + I-infected mice (Figures 7A and 7B). These axons were apparently wrapped in myelin sheath as revealed by myelin basic protein staining, suggesting that the iMN-projected axons could be packed as endogenous MN axons. To further investigate the progress of axonal projections after *Ngn2-Isl1* induced *in vivo* conversion in the hGFAP-CreERT2;Rosa-tdTomato mice spinal cord, we injected a retrograde tracer, cholera toxin subunit B (CTB), into the sciatic nerve at 42 dpi. The mice were sacrificed 7 days after CTB injection for analysis of the CTB-labeled neurons in the lumbar segment of the spinal cord. We found that numerous converted neurons ($NeuN^+/tdT^+/GFP^+$) in the lumbar segment were retrogradely labeled with CTB signal and besides, CTB was also detected in virus-infected endogenous neurons ($NeuN^+/tdT^-/GFP^+$) as expected (Figure 7C). Immunostaining

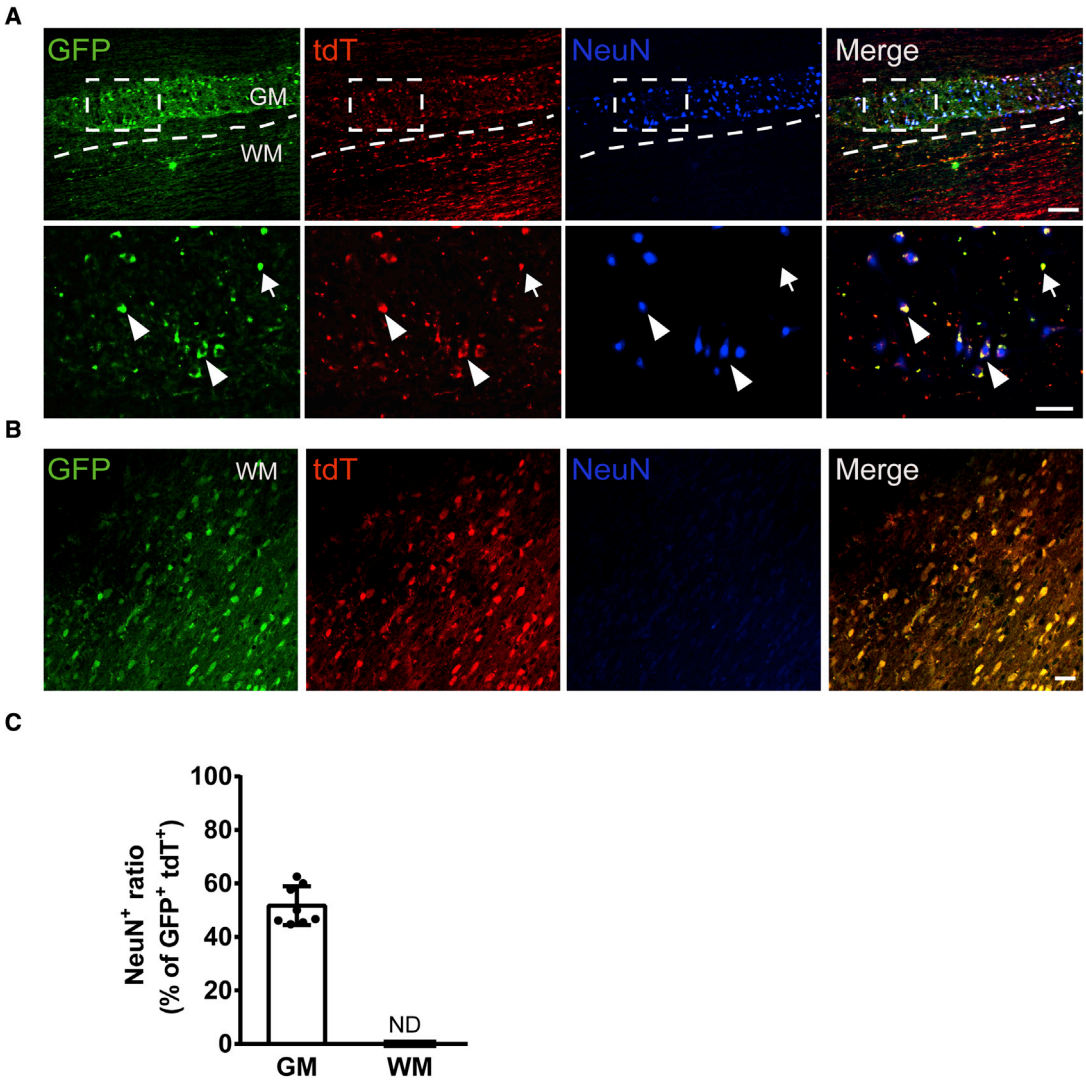

Figure 6. Astrocytes in the white matter of the spinal cord failed to convert to neurons

(A) Representative images showing the expression of the neuronal marker NeuN (42 dpi) in the gray matter (GM) region. Arrowheads indicate GFP^+/tdT^+ astrocyte-converted neurons. Arrows indicate the non-converted GFP^+/tdT^+ astrocytes. Scale bars, 200 μm (upper panels) and 50 μm (lower panels, high magnification).

(B) Representative images showing that no GFP^+/tdT^+ cells express the neuronal marker NeuN (42 dpi) in the white matter (WM) region. Scale bar, 20 μm.

(C) Quantified data showing the reprogramming efficiency in the GM and WM regions (n = 4 independent experiments). ND, not detected. Data are presented as mean ± SEM.

results of HB9 and ChAT further confirmed that CTB-labeled converted neurons are $HB9^+$ and $ChAT^+$ MNs (Figures S7A–S7C). Quantified data showed that 36% of the CTB-labeled neurons were converted iMNs, and 66% of the converted iMNs could be labeled with CTB (n = 4 mice, Figure 7D), indicating that these converted iMNs had projected into sciatic nerves. Altogether, these data suggest that the *in vivo* converted iMNs in the spinal cord could extend their axonal projections into the sciatic nerve to innervate target skeletal muscles.

DISCUSSION

Many nervous system diseases are associated with severe neuronal loss. How to replenish the lost neurons to restore function has proved to be a challenging task in the past. Previous studies have reported that there are newly formed neurons in the adult spinal cord, whether in physiological or pathological conditions (Noristani et al., 2016; Shechter et al., 2007), but other studies have shown that the adult spinal cord is not a neurogenic region and cannot produce new

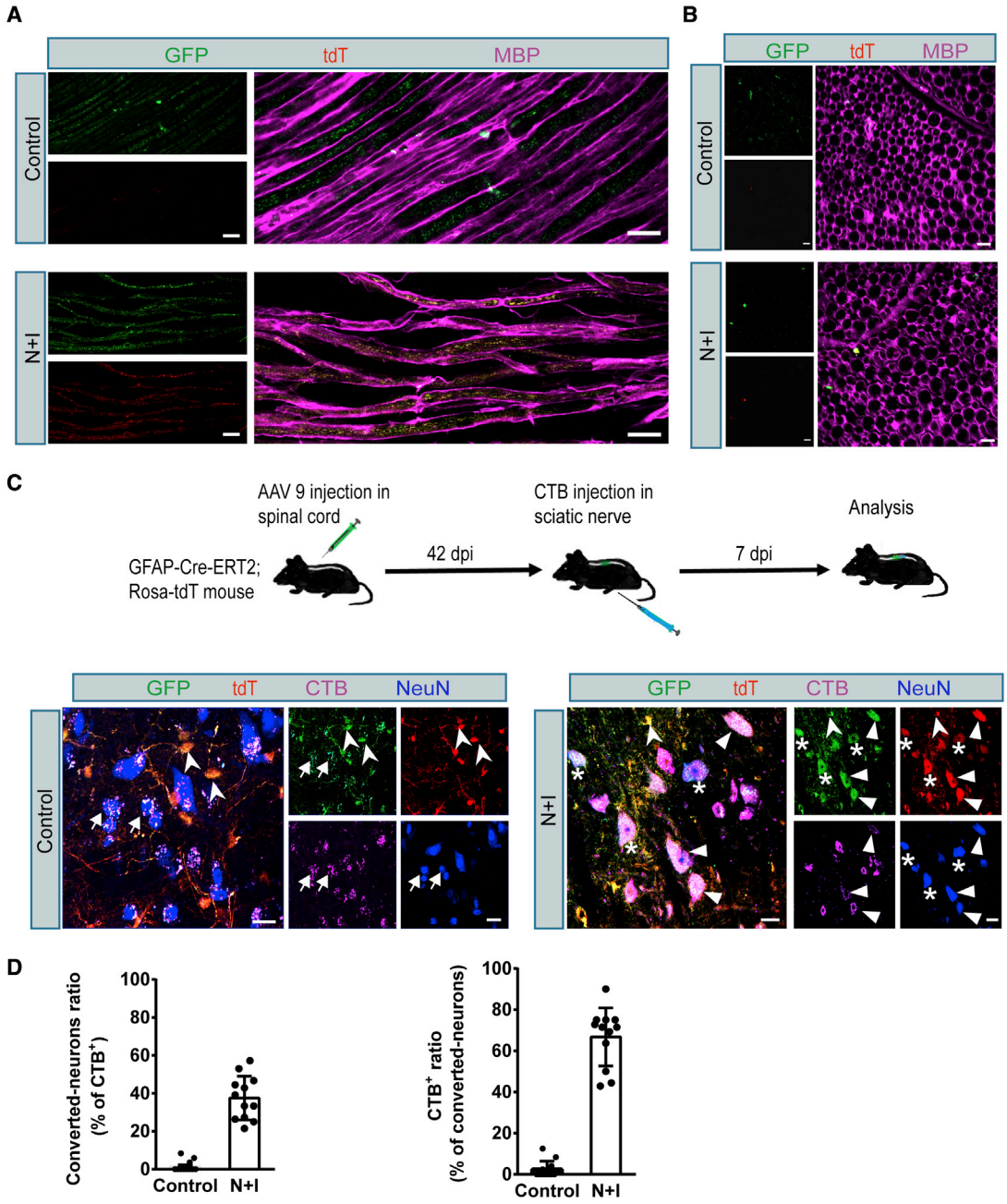

Figure 7. Axonal projections of the spinal cord astrocyte-converted neurons in the hGFAP-CreERT2;Ai14 mouse sciatic nerve

(A) High-resolution images showing GFP^+/tdT^+ axons co-stained with myelin basic protein (MBP) (bottom row) in sciatic nerve (42 dpi, longitudinal section). Scale bars, 20 μm.

(B) Representative images showing GFP^+/tdT^+ axons co-stained with MBP in sciatic nerve (42 dpi, cross-section). Scale bars, 10 μm.

(C) Retrograde tracing of spinal cord astrocyte-converted neurons by injecting CTB into the sciatic nerve at 42 dpi. CTB-labeled (purple) converted neurons ($GFP^+/tdT^+/NeuN^+$) were detected in the lumbar segment of spinal cord (arrowheads); viral infected endogenous neurons (arrows, $NeuN^+/tdT^-/GFP^+$) were retrogradely labeled by CTB, as expected. Stars indicate converted neurons not labeled with CTB ($tdT^+/GFP^+/NeuN^+/CTB^-$). Swallow-tail arrowheads indicate non-converted viral infected astrocytes ($tdT^+/GFP^+/CTB^-/NeuN^-$). Scale bars, 20 μm.

(D) Quantified data showing the percentage of CTB-labeled converted neurons in the lumbar segment of the spinal cord (n = 4 independent experiments). Data are presented as mean ± SEM.

neurons in the injured or uninjured state (Johansson et al., 1999; Ohori et al., 2006; Su et al., 2014). We also could not detect any newly produced neurons in the adult spinal cord with an injection of control AAV (Figure 4). Despite these debates, spontaneous neurogenesis in the adult spinal cord is extremely limited, so strategies are needed to overcome this limitation. As an alternative strategy, our present study illustrates that astrocytes can be reprogrammed into mature MNs in the adult spinal cord by CRISPRa-mediated activation of endogenous *Ngn2* and *Isl1*.

In this study, we demonstrated that activation of only two TFs, *Ngn2* and *Isl1*, by the CRISPRa system could convert astrocytes of mouse spinal cord into functional MNs with high efficiency. CRISPRa-mediated endogenous neurogenic factor activation had been reported previously (Black et al., 2016; Zhou et al., 2018), but our study is the first to use CRISPRa-based technology to induce MNs. The iMNs expressed pan-neuron and MN-specific markers, fired APs, and formed synaptic connections. Furthermore, MEFs could also be converted into functional MNs.

Direct reprogramming of somatic cells to neurons is a novel approach to the treatment of nerve injury and degeneration. In the process of culture, some TFs that determine cell fate can initiate reprogramming (Yang et al., 2011). It has been shown that somatic cells such as astrocytes or fibroblasts could be directly converted into various types of neurons, including glutamatergic, dopaminergic, and cholinergic neurons, by different combinations of TFs (Caiazzo et al., 2011; Liu et al., 2013, 2015). Different combinations of small molecules have previously been used to stably reprogram human fibroblasts into neurons by *Ascl1* and *Ngn2*. The reprogramming efficiency was high, but the cell types of transformation were the mixture of GABAergic (20%), glutamatergic (35%), and other subtype-specific neurons. Interestingly, there were no cholinergic neurons (Ladewig et al., 2012). *Ascl1* and *Ngn2* play different roles in cell-fate determination in different brain regions and spinal cord regions, among which *Ascl1* has the characteristics of indicative determinant and *Ngn2* is a permissive factor, which must be combined with other factors to determine the phenotype of neurons (Jo et al., 2007; Parras et al., 2002). The final balance of these two factors in heterogeneous cell groups may be the basis of mixed induction of neural subtypes. It was reported that fibroblasts could be induced into MNs through overexpressing seven TFs (*Ascl1*, *Brn2*, *Myt1l*, *Lhx3*, *Hb9*, *Isl1*, and *Ngn2*), but the reprogramming efficiency was not particularly satisfying (Son et al., 2011). *Isl1* and *Lhx3* are two important TFs for MN specification (Lee and Pfaff, 2001). It has been reported that *Ngn2* possessed the ability of reprogramming, directly converting human fibroblasts to cholinergic neurons when overexpressed together with the other three TFs *Sox11*, *Isl1*, and *Lhx3* (Liu et al., 2016). In the current study, we examined the effects of the combinatorial activation of four related TFs, *Ascl1*, *Ngn2*, *Lhx3*, and *Isl1*. To our surprise, spinal cord astrocytes could be converted into Tuj1$^+$/HB9$^+$ MNs without the activation of *Lhx3*. This observation may suggest that *Lhx3* is dispensable for MN reprogramming. We also found that double activation of *Ngn2* and *Isl1* was sufficient to efficiently convert MEFs and astrocytes from the spinal cord into iMNs *in vitro* and that these iMNs could form functional synapses (Figures 1, 2, and 3). Besides, activation of *Ascl1* and *Isl1* could also reprogram astrocytes into MNs (data not shown). This not only provides an alternative approach to direct neural reprogramming but also provides insights into the molecular mechanism of MN induction. The reprogramming efficiency from spinal cord astrocytes into iMNs was over 70%, which was higher than that from MEFs (64%). This may reflect the different distances of developmental lineages between astrocytes and fibroblasts. We evaluated the efficiency of iMN conversion by calculating the percentage of ChAT-positive cells, and the percentage of HB9$^+$ cells was comparable in iMNs converted from both initiating cells (~83%). Furthermore, iMNs induced by *Ngn2* and *Isl1* scarcely expressed the GABAergic neuronal marker.

AAVs are the most promising method for *in vivo* gene delivery. The length of time necessary to detect gene expression mediated by recombinant AAV is highly correlated with the type of virus used. Some recombinant AAVs provide fast and stable expression within 1 week while others need 2–4 weeks to reach maximum expression in the brain (Mason et al., 2010; Thevenot et al., 2012). In this study, we examined the reprogramming of astrocytes at different times after virus injection. We found that the expression of GFP was first detected at 14 days after AAV injection, but astrocyte-converted neurons were rarely detectable until 28 dpi. The reprogramming time is similar to that of induction *in vitro*. Our results demonstrated that the CRISPRa-mediated activation of *Ngn2* and *Isl1* could convert astrocytes into MNs with relatively higher efficiency (~44%) than that of *Sox2*-mediated astrocytes-to-MNs *in vivo* reprogramming (~8%) (Su et al., 2014). The divergence between the previous report and our study could be ascribed to differences in species, viral vector, and injury conditions used in these studies. Although the Cre expression may leak to neurons at the early developmental stage to some extent in hGFAP-CreERT2 transgenic mice, most tdT-labeled cells (>95%) are GFAP$^+$ astrocytes. This excluded the possibility of endogenous MNs as the main contributors to iMNs. Regional specification may pose hurdles to inducing neurons from other regions. A previous study reported that astrocytes fail to convert into neurons in the WM of the brain (Mattugini et al., 2019). In our study, astrocytes in the WM of the spinal cord also failed to be reprogrammed into neurons. These observations may suggest

that the surrounding environment plays a crucial role in cell-fate determination (Farmer et al., 2016).

It is worth noting that we cannot exclude the possibility that other MN-inducing factors are overlooked or that changing the mixture of the TF may further improve the converting efficiency and even the converting accuracy. Such a reprogramming method will significantly promote the generation of patient-specific MNs, which can be used in regenerative medicine as well as disease-related studies. For the modeling of MN-related diseases and cell-based therapy, a detailed understanding of the mechanism of iMN production will be crucial. Although we have successfully reprogrammed astrocytes into MNs by CRISPRa-mediated activation of endogenous target genes *in vivo*, there are still many important problems that remain to be solved. It will be of great significance to study whether different subtypes of neurons can be effectively induced *in vivo*, and whether the induced neurons can integrate into neural circuits and rescue the functional defects. Our current study provides a basis for the cell replacement therapy of motor nerve-related diseases and may also help to establish a cellular model for MN-related diseases through the conversion of patients' endogenous glial cells or fibroblasts to MNs.

EXPERIMENTAL PROCEDURES

A detailed description of all materials and methods is presented in supplemental experimental procedures.

Animals

Wild-type C57/BL6J mice were purchased from the Experimental Animal Center of Tongji Medical College, Huazhong University of Science and Technology. The Rosa26-CAG-tdTomato (Ai14) mice were kindly donated by Prof. Yan Zhou (Wuhan University) and obtained from The Jackson Laboratory (Madisen et al., 2010). The hGFAP-CreERT2 mice were obtained from MMRRC (Casper et al., 2007). Induction of expression of Cre in hGFAP-CreERT2;Ai14 transgenic mice was performed as previously described (Feng et al., 2018) with modifications. A detailed description of the methods is presented in supplemental experimental procedures. All animal care and experimental procedures complied with local and international guidelines on the ethical use of animals and were approved by The University Animal Welfare Committee, Tongji Medical College, Huazhong University of Science and Technology.

AAV injection

A laminectomy was performed to expose the dorsal spinal cord of T9–T11 segments, viruses (recombinant AAV stocks, serotype 9) were then injected into the spinal cord parenchyma at each of the two locations to the left and right of the position of the centerline, and 1 μL of virus (1.4×10^{12} vector genomes/mL, 1:1 mixture of AAV-dCas9-VP64-EGFP and AAV-sgRNAs) was injected into each site at a speed of 100 nL/min. After each injection, the pipette was left in the tissue for 10 min before being withdrawn slowly. The injecting pipette was pulled from a glass tube with a tip opening size of 18–20 μm in diameter. After injection, animals were returned to their homes for standard husbandry.

Retrograde tracing with cholera toxin B: injection into the sciatic nerve

For retrograde tracing, a 0.5% solution of Alexa Fluor 647-labeled CTB (Invitrogen) in PBS was injected into the sciatic nerves of the hGFAP-CreERT2;Ai14 transgenic mice at 42 days after AAV injection. The mice were anesthetized with ketamine/xylazine (100 mg/kg ketamine; 10 mg/kg xylazine). CTB was injected into the sciatic nerves using a Hamilton syringe and a 30-gauge needle. The injection volume was 1 μL. After injection, the needle was kept in place for at least 2 min before being withdrawn slowly. After 7 days of CTB injection, the mice were sacrificed for analysis of the CTB-labeled neurons in the lumbar segment of the spinal cord.

Statistical analysis

GraphPad Prism 7.0 software was used for statistical analysis charting. All results were presented as the mean ± SEM unless otherwise stated. The significance of the difference was determined using one way-ANOVA. $p < 0.05$ was considered statistically significant. All experiments were repeated three or more times.

SUPPLEMENTAL INFORMATION

Supplemental information can be found online at https://doi.org/10.1016/j.stemcr.2021.05.020.

AUTHOR CONTRIBUTIONS

M.Z., Y.Z., J.L., Y.M., L.-Q.Z., F.W., and B.Z. conceived the project and designed the study; M.S., M.C., D.L., B.W., and T.W. performed the experiments; M.Z., X.T., and B.Z. analyzed data; M.Z. drafted the manuscript; B.Z. edited the manuscript.

ACKNOWLEDGMENTS

We thank Dr. Yan Zhou (Wuhan University) for the gift of the Ai14 reporter mouse, Dr. Fang Zheng and Dr. Cheng Zhan for providing the hGFAP-CreERT2 mice, and Dr. Man Jiang for AAV packaging vectors. We thank all members of the Zhang laboratory for helpful discussions. This study was supported by the National Natural Science Foundation of China 81471283 (B.Z.) and the Fundamental Research Funds for the Central Universities, HUST: 2015QT007 (L.-Q.Z. and B.Z.).

Received: January 18, 2021
Revised: May 27, 2021
Accepted: May 27, 2021
Published: June 24, 2021

REFERENCES

Arbab, M., Baars, S., and Geijsen, N. (2014). Modeling motor neuron disease: the matter of time. Trends Neurosci. *37*, 642–652.

Bailey, R.M., Rozenberg, A., and Gray, S.J. (2020). Comparison of high-dose intracisterna magna and lumbar puncture intrathecal delivery of AAV9 in mice to treat neuropathies. Brain Res. *1739*, 146832.

Black, J.B., Adler, A.F., Wang, H.-G., D'Ippolito, A.M., Hutchinson, H.A., Reddy, T.E., Pitt, G.S., Leong, K.W., and Gersbach, C.A. (2016). Targeted epigenetic remodeling of endogenous loci by CRISPR/Cas9-Based transcriptional activators directly converts fibroblasts to neuronal cells. Cell Stem Cell *19*, 406–414.

Bradbury, E.J., and McMahon, S.B. (2006). Spinal cord repair strategies: why do they work? Nat. Rev. Neurosci. *7*, 644–653.

Caiazzo, M., Dell'Anno, M.T., Dvoretskova, E., Lazarevic, D., Taverna, S., Leo, D., Sotnikova, T.D., Menegon, A., Roncaglia, P., Colciago, G., et al. (2011). Direct generation of functional dopaminergic neurons from mouse and human fibroblasts. Nature *476*, 224–227.

Casper, K.B., Jones, K., and McCarthy, K.D. (2007). Characterization of astrocyte-specific conditional knockouts. Genesis *45*, 292–299.

Chen, H., Qian, K., Du, Z., Cao, J., Petersen, A., Liu, H., Blackbourn, L.W.t., Huang, C.L., Errigo, A., Yin, Y., et al. (2014). Modeling ALS with iPSCs reveals that mutant SOD1 misregulates neurofilament balance in motor neurons. Cell Stem Cell *14*, 796–809.

Chen, Y.C., Ma, N.X., Pei, Z.F., Wu, Z., Do-Monte, F.H., Keefe, S., Yellin, E., Chen, M.S., Yin, J.C., Lee, G., et al. (2020). A NeuroD1 AAV-based gene therapy for functional brain repair after ischemic injury through in vivo astrocyte-to-neuron conversion. Mol. Ther. *28*, 217–234.

Condorelli, D.F., Dell'Albani, P., Conticello, S.G., Barresi, V., Nicoletti, V.G., Caruso, A., Kahn, M., Vacanti, M., Albanese, V., de Vellis, J., et al. (1997). A neural-specific hypomethylated domain in the 5′ flanking region of the glial fibrillary acidic protein gene. Dev. Neurosci. *19*, 446–456.

Cong, L., Ran, F.A., Cox, D., Lin, S., Barretto, R., Habib, N., Hsu, P.D., Wu, X., Jiang, W., Marraffini, L.A., et al. (2013). Multiplex genome engineering using CRISPR/Cas systems. Science *339*, 819–823.

Courtine, G., and Sofroniew, M.V. (2019). Spinal cord repair: advances in biology and technology. Nat. Med. *25*, 898–908.

Drouin-Ouellet, J., Pircs, K., Barker, R.A., Jakobsson, J., and Parmar, M. (2017). Direct neuronal reprogramming for disease modeling studies using patient-derived neurons: what have we learned? Front. Neurosci. *11*, 530.

Farmer, W.T., Abrahamsson, T., Chierzi, S., Lui, C., Zaelzer, C., Jones, E.V., Bally, B.P., Chen, G.G., Théroux, J.-F., Peng, J., et al. (2016). Neurons diversify astrocytes in the adult brain through sonic hedgehog signaling. Science *351*, 849–854.

Fawcett, J.W., and Asher, R.A. (1999). The glial scar and central nervous system repair. Brain Res. Bull. *49*, 377–391.

Fehlings, M.G., Tetreault, L.A., Wilson, J.R., Kwon, B.K., Burns, A.S., Martin, A.R., Hawryluk, G., and Harrop, J.S. (2017). A clinical practice guideline for the management of acute spinal cord injury: introduction, rationale, and scope. Glob. Spine J. *7*, 84s–94s.

Feng, J., Luo, J., Yang, P., Du, J., Kim, B.S., and Hu, H. (2018). Piezo2 channel-Merkel cell signaling modulates the conversion of touch to itch. Science *360*, 530–533.

Fernandopulle, M.S., Prestil, R., Grunseich, C., Wang, C., Gan, L., and Ward, M.E. (2018). Transcription factor-mediated differentiation of human iPSCs into neurons. Curr. Protoc. Cell Biol. *79*, e51.

Furlan, A., La Manno, G., Lübke, M., Häring, M., Abdo, H., Hochgerner, H., Kupari, J., Usoskin, D., Airaksinen, M.S., Oliver, G., et al. (2016). Visceral motor neuron diversity delineates a cellular basis for nipple- and pilo-erection muscle control. Nat. Neurosci. *19*, 1331–1340.

Gong, Z., Xia, K., Xu, A., Yu, C., Wang, C., Zhu, J., Huang, X., Chen, Q., Li, F., and Liang, C. (2020). Stem cell transplantation: a promising therapy for spinal cord injury. Curr. Stem Cell Res. Ther. *15*, 321–331.

Heinrich, C., Blum, R., Gascón, S., Masserdotti, G., Tripathi, P., Sánchez, R., Tiedt, S., Schroeder, T., Götz, M., and Berninger, B. (2010). Directing astroglia from the cerebral cortex into subtype specific functional neurons. PLoS Biol. *8*, e1000373.

Herdy, J., Schafer, S., Kim, Y., Ansari, Z., Zangwill, D., Ku, M., Paquola, A., Lee, H., Mertens, J., and Gage, F.H. (2019). Chemical modulation of transcriptionally enriched signaling pathways to optimize the conversion of fibroblasts into neurons. eLife *8*, e41356.

Jo, A.Y., Park, C.H., Aizawa, S., and Lee, S.H. (2007). Contrasting and brain region-specific roles of neurogenin2 and mash1 in GABAergic neuron differentiation in vitro. Exp. Cell Res. *313*, 4066–4081.

Johansson, C.B., Momma, S., Clarke, D.L., Risling, M., Lendahl, U., and Frisen, J. (1999). Identification of a neural stem cell in the adult mammalian central nervous system. Cell *96*, 25–34.

Klim, J.R., Williams, L.A., Limone, F., Guerra San Juan, I., Davis-Dusenbery, B.N., Mordes, D.A., Burberry, A., Steinbaugh, M.J., Gamage, K.K., Kirchner, R., et al. (2019). ALS-implicated protein TDP-43 sustains levels of STMN2, a mediator of motor neuron growth and repair. Nat. Neurosci. *22*, 167–179.

Knoepfler, P.S. (2009). Deconstructing stem cell tumorigenicity: a roadmap to safe regenerative medicine. Stem Cells *27*, 1050–1056.

Konermann, S., Brigham, M.D., Trevino, A.E., Joung, J., Abudayyeh, O.O., Barcena, C., Hsu, P.D., Habib, N., Gootenberg, J.S., Nishimasu, H., et al. (2015). Genome-scale transcriptional activation by an engineered CRISPR-Cas9 complex. Nature *517*, 583–588.

Ladewig, J., Mertens, J., Kesavan, J., Doerr, J., Poppe, D., Glaue, F., Herms, S., Wernet, P., Kögler, G., Müller, F.-J., et al. (2012). Small molecules enable highly efficient neuronal conversion of human fibroblasts. Nat. Methods *9*, 575–578.

Lee, S.-K., and Pfaff, S.L. (2001). Transcriptional networks regulating neuronal identity in the developing spinal cord. Nat. Neurosci. *4*, 1183–1191.

Li, S., Shi, Y., Yao, X., Wang, X., Shen, L., Rao, Z., Yuan, J., Liu, Y., Zhou, Z., Zhang, Z., et al. (2019). Conversion of astrocytes and fibroblasts into functional noradrenergic neurons. Cell Rep. *28*, 682–697.e7.

Liu, M.L., Zang, T., and Zhang, C.L. (2016). Direct lineage reprogramming reveals disease-specific phenotypes of motor neurons from human ALS patients. Cell Rep. *14*, 115–128.

Liu, M.L., Zang, T., Zou, Y., Chang, J.C., Gibson, J.R., Huber, K.M., and Zhang, C.L. (2013). Small molecules enable neurogenin 2 to efficiently convert human fibroblasts into cholinergic neurons. Nat. Commun. *4*, 2183.

Liu, P., Chen, M., Liu, Y., Qi, L.S., and Ding, S. (2018). CRISPR-based chromatin remodeling of the endogenous Oct4 or Sox2 locus enables reprogramming to pluripotency. Cell Stem Cell *22*, 252–261.e4.

Liu, Y., Miao, Q., Yuan, J., Han, S., Zhang, P., Li, S., Rao, Z., Zhao, W., Ye, Q., Geng, J., et al. (2015). Ascl1 converts dorsal midbrain astrocytes into functional neurons in vivo. J. Neurosci. *35*, 9336–9355.

Lykken, E.A., Shyng, C., Edwards, R.J., Rozenberg, A., and Gray, S.J. (2018). Recent progress and considerations for AAV gene therapies targeting the central nervous system. J. Neurodev. Disord. *10*, 16.

Madisen, L., Zwingman, T.A., Sunkin, S.M., Oh, S.W., Zariwala, H.A., Gu, H., Ng, L.L., Palmiter, R.D., Hawrylycz, M.J., Jones, A.R., et al. (2010). A robust and high-throughput Cre reporting and characterization system for the whole mouse brain. Nat. Neurosci. *13*, 133–140.

Mali, P., Yang, L., Esvelt, K.M., Aach, J., Guell, M., DiCarlo, J.E., Norville, J.E., and Church, G.M. (2013). RNA-guided human genome engineering via Cas9. Science *339*, 823–826.

Mason, M.R., Ehlert, E.M., Eggers, R., Pool, C.W., Hermening, S., Huseinovic, A., Timmermans, E., Blits, B., and Verhaagen, J. (2010). Comparison of AAV serotypes for gene delivery to dorsal root ganglion neurons. Mol. Ther. *18*, 715–724.

Mattugini, N., Bocchi, R., Scheuss, V., Russo, G.L., Torper, O., Lao, C.L., and Gotz, M. (2019). Inducing different neuronal subtypes from astrocytes in the injured mouse cerebral cortex. Neuron *103*, 1086–1095.e5.

Noristani, H.N., Sabourin, J.C., Boukhaddaoui, H., Chan-Seng, E., Gerber, Y.N., and Perrin, F.E. (2016). Spinal cord injury induces astroglial conversion towards neuronal lineage. Mol. Neurodegener. *11*, 68.

Ohori, Y., Yamamoto, S., Nagao, M., Sugimori, M., Yamamoto, N., Nakamura, K., and Nakafuku, M. (2006). Growth factor treatment and genetic manipulation stimulate neurogenesis and oligodendrogenesis by endogenous neural progenitors in the injured adult spinal cord. J. Neurosci. *26*, 11948–11960.

Parras, C.M., Schuurmans, C., Scardigli, R., Kim, J., Anderson, D.J., and Guillemot, F. (2002). Divergent functions of the proneural genes Mash1 and Ngn2 in the specification of neuronal subtype identity. Genes Dev. *16*, 324–338.

Polstein, L.R., Perez-Pinera, P., Kocak, D.D., Vockley, C.M., Bledsoe, P., Song, L., Safi, A., Crawford, G.E., Reddy, T.E., and Gersbach, C.A. (2015). Genome-wide specificity of DNA binding, gene regulation, and chromatin remodeling by TALE- and CRISPR/Cas9-based transcriptional activators. Genome Res. *25*, 1158–1169.

Qian, H., Kang, X., Hu, J., Zhang, D., Liang, Z., Meng, F., Zhang, X., Xue, Y., Maimon, R., Dowdy, S.F., et al. (2020). Reversing a model of Parkinson's disease with in situ converted nigral neurons. Nature *582*, 550–556.

Shechter, R., Ziv, Y., and Schwartz, M. (2007). New GABAergic interneurons supported by myelin-specific T cells are formed in intact adult spinal cord. Stem Cells *25*, 2277–2282.

Snyder, E.Y., and Teng, Y.D. (2012). Stem cells and spinal cord repair. N. Engl. J. Med. *366*, 1940–1942.

Son, E.Y., Ichida, J.K., Wainger, B.J., Toma, J.S., Rafuse, V.F., Woolf, C.J., and Eggan, K. (2011). Conversion of mouse and human fibroblasts into functional spinal motor neurons. Cell Stem Cell *9*, 205–218.

Su, Z., Niu, W., Liu, M.L., Zou, Y., and Zhang, C.L. (2014). In vivo conversion of astrocytes to neurons in the injured adult spinal cord. Nat. Commun. *5*, 3338.

Teter, B., Rozovsky, I., Krohn, K., Anderson, C., Osterburg, H., and Finch, C. (1996). Methylation of the glial fibrillary acidic protein gene shows novel biphasic changes during brain development. Glia *17*, 195–205.

Thevenot, E., Jordao, J.F., O'Reilly, M.A., Markham, K., Weng, Y.Q., Foust, K.D., Kaspar, B.K., Hynynen, K., and Aubert, I. (2012). Targeted delivery of self-complementary adeno-associated virus serotype 9 to the brain, using magnetic resonance imaging-guided focused ultrasound. Hum. Gene Ther. *23*, 1144–1155.

Thuret, S., Moon, L.D., and Gage, F.H. (2006). Therapeutic interventions after spinal cord injury. Nat. Rev. Neurosci. *7*, 628–643.

Vadodaria, K.C., Mertens, J., Paquola, A., Bardy, C., Li, X., Jappelli, R., Fung, L., Marchetto, M.C., Hamm, M., Gorris, M., et al. (2016). Generation of functional human serotonergic neurons from fibroblasts. Mol. Psychiatr. *21*, 49–61.

Vierbuchen, T., Ostermeier, A., Pang, Z.P., Kokubu, Y., Südhof, T.C., and Wernig, M. (2010). Direct conversion of fibroblasts to functional neurons by defined factors. Nature *463*, 1035–1041.

Xu, Z., Jiang, H., Zhong, P., Yan, Z., Chen, S., and Feng, J. (2016). Direct conversion of human fibroblasts to induced serotonergic neurons. Mol. Psychiatr. *21*, 62–70.

Yang, N., Ng, Y.H., Pang, Z.P., Sudhof, T.C., and Wernig, M. (2011). Induced neuronal cells: how to make and define a neuron. Cell Stem Cell *9*, 517–525.

Yiu, G., and He, Z. (2006). Glial inhibition of CNS axon regeneration. Nat. Rev. Neurosci. *7*, 617–627.

Zalatan, J.G., Lee, M.E., Almeida, R., Gilbert, L.A., Whitehead, E.H., La Russa, M., Tsai, J.C., Weissman, J.S., Dueber, J.E., Qi, L.S., et al. (2015). Engineering complex synthetic transcriptional programs with CRISPR RNA scaffolds. Cell *160*, 339–350.

Zhou, H., Liu, J., Zhou, C., Gao, N., Rao, Z., Li, H., Hu, X., Li, C., Yao, X., Shen, X., et al. (2018). In vivo simultaneous transcriptional activation of multiple genes in the brain using CRISPR–dCas9-activator transgenic mice. Nat. Neurosci. *21*, 440–446.

Zhou, H., Su, J., Hu, X., Zhou, C., Li, H., Chen, Z., Xiao, Q., Wang, B., Wu, W., Sun, Y., et al. (2020). Glia-to-Neuron conversion by CRISPR-CasRx alleviates symptoms of neurological disease in mice. Cell *181*, 590–603.e16.